# Characterization of Diodes in a Coaxial Measurement System

Michael B. Steer[1] and Ross G. Hicks[2]

[1] High Frequency Electronics Laboratory
Department of Electrical and Computer Engineering
North Carolina State University
Raleigh, North Carolina 27695-7911, U.S.A.

[2]Compact Software, 483 McLean Boulevard, Paterson, New Jersey 07504, U.S.A.

ABSTRACT

A method is reported for experimentally characterizing packaged microwave diodes with respect to their outer cylindrical surface. The diode is mounted coaxial with the center conductor of a coaxial line and radial transmission line theory is used to determine the impedance of dummy diode packages used in calibration. The diode equivalent circuit thus developed is suited to the modeling of a diode mounted in a post-in-waveguide mount. Experimental characterization of a varactor diode and of a mixer diode are reported.

## I. INTRODUCTION

Post-in-waveguide diode mounts [1] – [4] present a radial electromagnetic field to the cylindrical surface of a packaged diode. Accurate diode equivalent circuits, referred to the radial modes at the cylindrical surface, are required to take full advantage of recent advances in the modeling of these mounts [4].

Diodes have previously been characterized mounted in coaxial lines [5] – [8] and in reduced height waveguide [9] – [11], De Loach [11] uses narrow-band transmission resonance measurements to determine the elements of an assumed diode equivalent circuit. Most, however, [5] – [10], use a standard three-termination calibration procedure to determine the error two-port between the measurement plane and the cylindrical surface of the diode. Standard impedances, generally posts of varying diameters, are substituted for the diode. The actual impedance of the standards referred to the diode reference plane is calculated using radial line theory [12]. It is necessary, however, to keep the post diameters less than that of the coaxial center conductor to maintain the radial field distribution at what would be the surface of the diode. Removing the diode to present an open-circuit significantly alters the field distribution in the vicinity of the mount and so can not be used to present a calibrated impedance. Thus only a narrow range of impedances can be used during calibration. In this paper we use a coaxial diode mount and introduce a plexi-glass loaded package to obtain a high impedance termination and still maintain field orientation. Again radial line theory is used to determine the actual impedance presented at the diode reference plane. Varactor and mixer diodes are experimentally characterized using small signal microwave measurements together with low frequency capacitance versus voltage and dc current versus voltage measurements. The radial field orientation during the ac measurements is determined to be adequate by also considering a modified coaxial mount which enhances the establishment of radial fields in the vicinity of the diode. The diode equivalent circuit thus developed is suited to the modeling of a diode in a post-in-waveguide mount.

Because of the small dimensions of the diode only the TEM radial mode is assumed to exist at the diode surface. The TEM radial mode has electric and magnetic fields which are perpendicular to the direction of propagation and will be tangential to the diode surface. This mode is also designated as $TM_{0,1,0}$ (where the subscripts describe the variations in the circumferential, radial and vertical directions respectively). Thus the coaxial line diode mount of Fig. 1 can be modeled as shown in Fig. 2 where AA is the network analyzer measurement port, BB is a diode reference port and CC is the diode surface. Non-TEM radial modes will exist in the transition from the coaxial TEM mode to the TEM radial mode but, provided the field orientation does not change, the effect of these can be lumped into the embedding network.

The standard three-load calibration procedure enables the embedding network to be determined. The reference loads were obtained using the three dummy packages shown in Fig. 3 with Fig. 3(ii) showing the dummy packages mounted in the coaxial line diode mount. The impedances of the packages were obtained using the radial line equivalent circuits of the packages, Fig. 3(iii). The effect of the fringing fields arising from the coaxial mode to radial mode transition is not included in the dummy package models so that it is incorporated in the embedding network.

The input impedance of package (b) is traditionally obtained by approximating the package as a parallel plate capacitor. The input impedance of package (b) is the TEM mode input admittance of a disk This is derived from the principles presented in [13]. A radial line disk is a section of radial line extending from radius r to zero radius. The standing wave forms of the equivalent voltages and currents of a TM section of radial line are [13]

$$V(r) = A_n J_n(k_c r) + B_n N_n(k_c r) \quad (1)$$

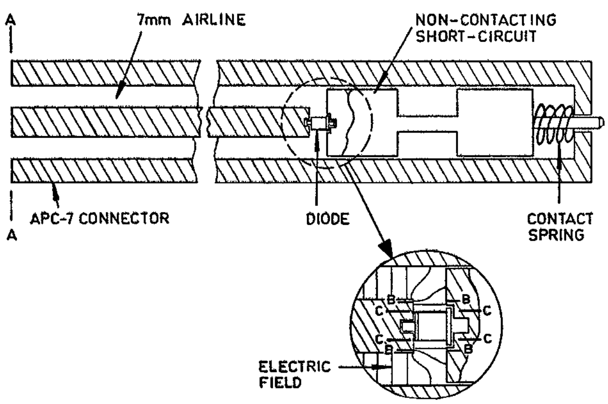


Figure 1: Coaxial line diode mount.

OF-I

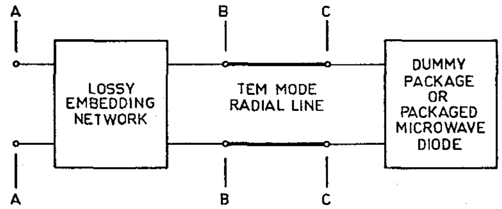


Figure 2: Components of the coaxial line diode mount.

and

$$I(r) = \jmath\left(\frac{2\pi\omega\epsilon}{bk_c}\right) r\frac{\epsilon_{0m}}{\epsilon_{0n}}\left(A_nJ_n'(k_cr) + B_nN_n'(k_cr)\right) \qquad (2)$$

where $J_n(x)$ and $N_n(x)$ are first and second kind bessel functions of order n respectively, $n$ and $m$ are the circumferential and axial varaiation indexes respectively, and $\epsilon_{0i}$ is Neumann's number ($\epsilon_{0i} = 1$ for $i = 0$; $\epsilon_{0i} = 2$ for $i/ = 0$). These equivalent volatage and current must be analytic at zero radius. Thus $B_n$ is zero as $N_n(k_cr)$ goes to negative infinity as r approaches zero and so the voltages and currents at a radius $r$, are

$$V(r) = A_nJ_n(k_cr) \qquad (3)$$

and

$$I(r) = \jmath\left(\frac{2\pi\omega\epsilon}{bk_c}\right) r\frac{\epsilon_{0m}}{\epsilon_{0n}}A_nJ_n'(k_cr) \qquad (4)$$

Hence the input admittance of the disc at radius $r_1$ (i.e. the admittance referred to the cylindrical surface at $r_1$ looking into the disc) is

$$Y_{\text{in}}(r_1) = \frac{I(r_1)}{V(r_1)} = \jmath\left(\frac{2\pi\omega\epsilon r_1}{bk_c}\right)\frac{\epsilon_{0m}}{\epsilon_{0n}}\frac{J_n'(k_cr_1)}{J_n(k_cr_1)} \qquad (5)$$

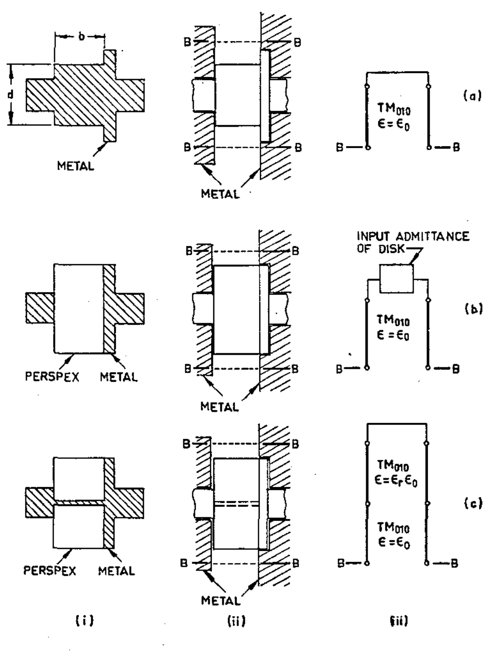


Figure 3: Reference loads: (i) dummy package, (ii) mounted package (iii) equivalent circuit of package; (a) brass package, (diameter, $d = 2.01$ mm and height, $b = 1.54$ mm); (b) plexi-glass (perspex) package, (diameter, $d = 3.1$ mm and height, $b = 1.54$ mm); and (c) plexi-glass package (diameter, $d = 3.06$ mm and height, $b = 1.54$ mm) with a thin coaxial brass pin of diameter 0.5 mm.

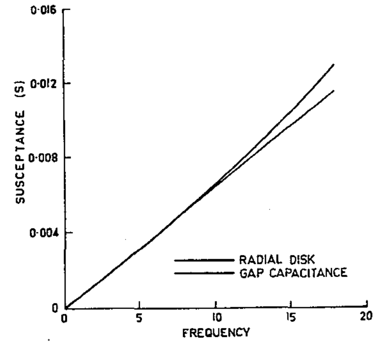


Figure 4: Comparison of the TEM radial-mode input susceptance of the plexi-glass package with the susceptance of a parallel plate capacitor with equivalent dimensions.

In Fig. 4, the input admittance of package (b) calculated using the parallel plate approximation, is compared to that obtained using the radial line model of the package. It can be seen that the parallel plate approximation is valid up to 10 GHz. However, above 10 GHz the error of the approximation becomes significant, reaching 10% at 18 GHz.

Measurements of the mounted diode were then deembedded to yield the input impedance of the diode. A large number of measurements enabled the use of minimization techniques to fit the assumed equivalent circuit of the diode to the measured data.

## III. Results

*Microwave measurements*

A Microwave Associates GaAs varactor diode in an S4 package was characterized assuming the equivalent circuit of the diode shown in Fig. 5 where $C_j = C_{j0}/(1 - v/\phi)$ and $R_j$ (described by $i = I_S[\exp(qv/\eta kT) - 1]$) model the semiconductor junction; $C_c$ results from the bias independent part of the junction capacitance and the capacitance of the package in the vicinity of the semiconductor; $R_S'$ is the diode series resistance due to the resistance of the undepleted semiconductor and contact resistance; and $L_p$ and $C_p$ are parasitic reactances of the package. The elements of the diode equivalent circuit were obtained by minimizing an impedance error function, a function of the calculated impedances of the diode model and the measured impedances of the diode [8] yielding, for the zero-biased diode: $C_p = 0.0545$ pF, $L_p = 0.416$ nH, $R_j > 10$ kΩ, $R_S = 1.42$ Ω and $C_j + C_c = 0.599$ pF. The impedance of the diode calculated using the equivalent circuit agrees closely with the measured impedance, as shown in Fig. 6. The diode was also characterized at 0.5 V bias yielding linear element ($C_p$, $L_p$ and $R_S$) values within 5% of the values determined at zero bias.

*Capacitance-voltage measurements*

The capacitance of the diode, for a range of bias voltages, was measured using a 1 MHz capacitance bridge. A nonlinear least squares technique [14] yielded the following equivalent circuit parameters (after allowing for a stray capacitance of 0.367 pF): $\phi = 1.088$ V, $\gamma = 0.4136$, $C_{j0} = 0.404$ pF, $C_p + C_c = 0.264$ pF and, in conjunction with the small signal microwave measurements of, $C_p = 0.055$ pF,

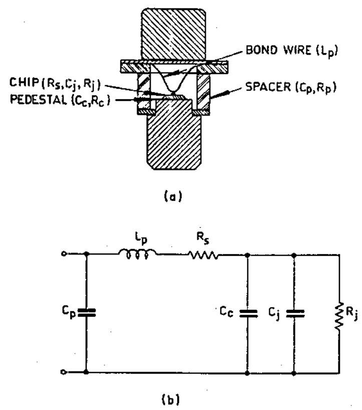


Figure 5: Varactor diode. (a) in an S4 package, (b) assumed equivalent circuit of diode.

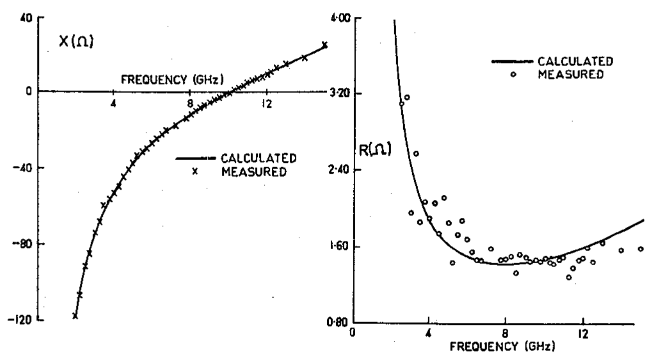


Figure 6: Comparison of the measured input impedance of the diode with that calculated using the diode equivalent circuit. Impedance = $R + jX$.

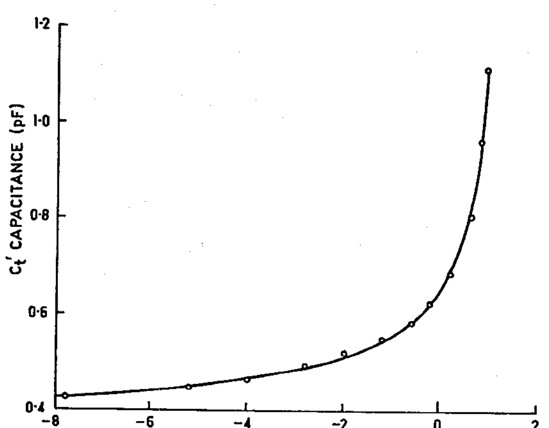


Figure 7: Comparison of the measured capacitance versus voltage characteristic of the diode and that calculated using the diode model.

$C_c$ = 0.210 pF. Fig. 7 indicates the excellent degree of fit between the measured and calculated capacitance versus voltage characteristic. The total diode capacitance at 1 MHz (0.668 pF at zero bias, 0.780 pF at .5 V bias) compares favorably to the total capacitance of the diode determined from microwave measurements (0.645 pF at zero bias, 0.767 pF at 0.5 V bias).

*Current-voltage measurement*

The parameters of the Shockley diode equation were determined graphically using current versus voltage measurements yielding: $I_s$ = 0.71 pA and $\eta$ = 1.93. The degree of fit of the calculated and measured current versus voltage characteristics is shown in Fig. 8.

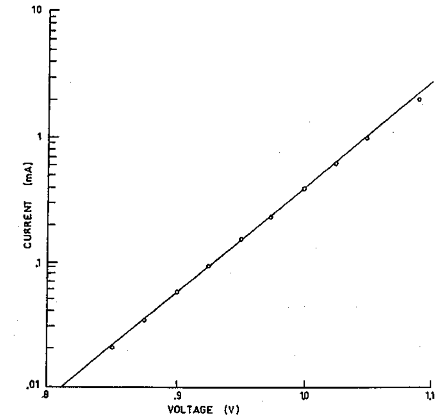


Figure 8: Comparison of the measured current versus voltage characteristic of the diode and that calculated using the diode model.

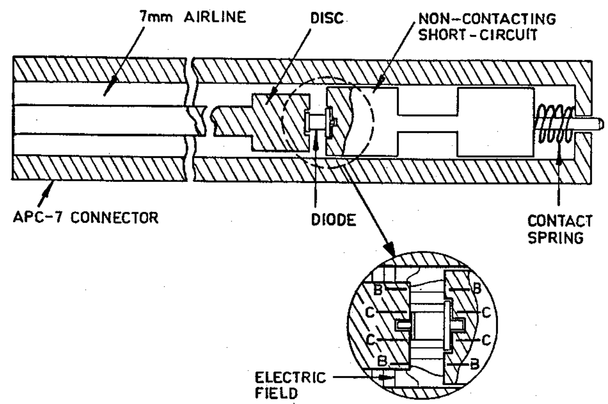


Figure 9: Enhanced radial mode coaxial line diode mount.

## IV. Discussion and Conclusion

A basic assumption of the mount schematic of Fig. 2, and thus a possible source of systematic error, is that the non-TEM radial modes at BB do not interact with the non-TEM radial modes at the diode surface, CC. This has been a common concern with this type of mount and the field distribution predicted to be that of a TEM coaxial mode by some workers [15]. To investigate the TEM radial mode assumption, the diode was also characterized using the enhanced radial mode, coaxial line diode mount of Fig. 9. The main feature of this mount is the longer radial transmission line surrounding the diode. Thus the non-TEM radial mode in the vicinity of the diode will be smaller than with the ordinary coaxial line mount of Fig. 1. The diode input impedances determined using the enhanced and ordinary mounts were within 4% over the full 2 to 18 GHz measurement range. This supports the assumption that the radial mode is fully developed in the radial line region of the coaxial mount of Fig. 1.

The agreement shown in Fig. 6 between the microwave measurements and the impedance of the diode equivalent circuit is very good. This level of agreement, however, is dependent on the characteristics of the diode. A schottky barrier mixer diode with the assumed equivalent circuit of Fig. 10 was also characterized. Again the diode equivalent circuit was obtained by minimizing an input impedance error function. The measured diode impoedance is compared to the calculated from the model in Fig. 11. The dispersion of the resistance is principally due to the larger reactive component of the diode. Clearly, as the reactive component reduces at higher frequencies, the resistance values portray less erratic behavior.

## References


[1] B. D. Bates, "Analysis of multiple-step radial-resonator waveguide diode mounts with application to IMPATT circuits," in *1987 IEEE MTT-S International Microwave Symposium Digest*, June 1987, pp. 669-672.

[2] M. E. Bialkowski, "Analysis of disc-type resonator mounts in parallel plate and rectangular waveguides," *Arch. Elek. Übertragung*, Vol. 38, No. 5, September/October 1984, pp. 306-310.

[3] A.C. Derycke and G. Salmer, "Circuit analysis and design of radial pretuned modules used for millimeter-wave oscillators," *IEEE Trans. Microwave Theory Tech.*, Vol. MTT-33, July 1985, pp. 600-609.

[4] B. D. Bates and A. Ko, "Modal analysis of radial-resonator waveguide diode mounts," *IEEE Trans. Microwave Theory Tech.*, Vol. MTT-38, August 1990, pp. 1037-1045.

[5] J.W. Bandler, "Precision microwave measurements of the internal parasitics of tunnel-diodes," *IEEE Trans. Electron Devices*, vol. ED-15, May 1968, pp. 275-282.

[6] D.R. Decker, C.N. Dunn, and R.L. Frank, "Large-signal silicon and germanium avalanche diode characteristics," *IEEE Trans. Microwave Theory Tech.*, vol. MTT-18, Nov. 1970, pp. 872-876.

[7] M. Ohtomo, "Broad-band small-signal impedance characterization of silicon (Si) P+-N-N+ IMPATT diodes," *IEEE Trans. Microwave Theory Tech.*, vol. MTT-22, July 1974, pp. 709-717.

[8] P.T. Greiling and R.W. Laton, "Determination of semiconductor junction device package networks," *IEEE Trans. Microwave Theory Tech.*, vol. MTT-22, Dec. 1974, pp. 1140-1145.

[9] J.M. Roe and F.J. Rosenbaum, "Characterization of packaged microwave diodes in reduced-height waveguide," *IEEE Trans. Microwave Theory Tech.*, vol. MTT-18, Sept. 1970, pp. 638-642.

[10] Y.S. Lee and W.J. Getsinger, "Characterization of packaged varactor diodes," *International Microwave Symposium Digest*, May 1971, pp. 42-43.

[11] B.C. DeLoach, "A new microwave measurement technique to characterize diodes and an 800-Gc cutoff frequency varactor at zero volts bias," *IEEE Trans. on Microwave Theory and Tech.*, Jan. 1964, pp. 15-20.

[12] N. Marcuvitz, "Radial transmission lines," in *Principles of Microwave Circuits*, C.G. Montgomery, R.H. Duke, and E.M. Purcell, Eds. (MIT Radiation Laboratory Series, vol. 8) New York:McGraw-Hill, 1947., pp. 240-282.

[13] M.B. Steer and P.J. Khan, "Wideband equivalent circuits for radial transmission lines," *Proc. IEE part H*, Vol. 128, No. 2, April 1981, pp. 111-113.

[14] R.D. Pollard, M.J. Howes, and D.V. Morgan, "Consideration of accuracy in the determination of the capacitance voltage law parameters of microwave diodes," *Proc. IEEE*, vol. 63, Feb. 1975, pp. 323-325.

[15] R.P. Owens and D. Cawsey, "Microwave equivalent-circuit parameters of Gunn-effect-device packages," *IEEE Trans. on Microwave Theory and Tech.*, vol. MTT-18, Nov. 1970, pp. 790-798.


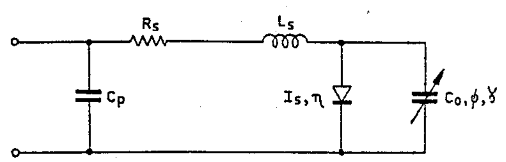


Figure 10: Schottky-barrier diode equivalent circuit.

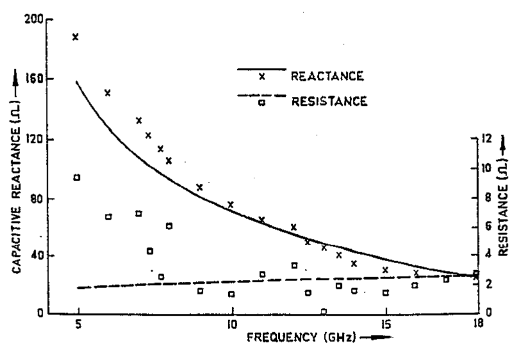


Figure 11: Comparison of microwave measurements (denoted ×, □) and results calculated using the diode equivalent circuit for the schottky barrier mixer diode.